Journal of Neurochemistry

JOURNAL OF NEUROCHEMISTRY | 2012 | 123 | 613–621

doi: 10.1111/j.1471-4159.2012.07936.x

ORIGINAL ARTICLE

Early mitochondrial abnormalities in hippocampal neurons cultured from *Fmr1* pre-mutation mouse model

Eitan S. Kaplan,*,[1] Zhengyu Cao,*,[1] Susan Hulsizer,* Flora Tassone,†,§ Robert F. Berman,‡,§ Paul J. Hagerman†,§ and Isaac N. Pessah*,§

*Department of Molecular Biosciences, School of Veterinary Medicine, University of California, Davis, California, USA

†Department of Biochemistry and Molecular Medicine, School of Medicine, University of California, Davis, California, USA

‡Department of Neurological Surgery, School of Medicine, University of California, Davis, California, USA

§Medical Investigations of Neurodevelopmental Disorders (MIND) Institute, University of California, Davis, California, USA

Abstract

Pre-mutation CGG repeat expansions (55–200 CGG repeats; pre-CGG) within the fragile-X mental retardation 1 (*FMR1*) gene cause fragile-X-associated tremor/ataxia syndrome in humans. Defects in neuronal morphology, early migration, and electrophysiological activity have been described despite appreciable expression of fragile-X mental retardation protein (FMRP) in a pre-CGG knock-in (KI) mouse model. The triggers that initiate and promote pre-CGG neuronal dysfunction are not understood. The absence of FMRP in a *Drosophila* model of fragile-X syndrome was shown to increase axonal transport of mitochondria. In this study, we show that dissociated hippocampal neuronal culture from pre-CGG KI mice (average 170 CGG repeats) express 42.6% of the FMRP levels and 3.8-fold higher *Fmr1* mRNA than that measured in wild-type neurons at 4 days *in vitro*. Pre-CGG hippocampal neurons show abnormalities in the number, mobility, and metabolic function of mitochondria at this early stage of differentiation. Pre-CGG hippocampal neurites contained significantly fewer mitochondria and greatly reduced mitochondria mobility. In addition, pre-CGG neurons had higher rates of basal oxygen consumption and proton leak. We conclude that deficits in mitochondrial trafficking and metabolic function occur despite the presence of appreciable FMRP expression and may contribute to the early pathophysiology in pre-CGG carriers and to the risk of developing clinical fragile-X-associated tremor/ataxia syndrome.

Keywords: autism, *Fmr1*, FXTAS, fragile-X, mitochondria, OCR.

J. Neurochem. (2012) **123**, 613–621.

Fragile-X-associated tremor/ataxia syndrome (FXTAS) is a late-onset neurodegenerative disorder that can occur in carriers of a trinucleotide (CGG) expansion (between 55 and 200 repeats; pre-mutation), within the 5′-non-coding region of the fragile-X mental retardation 1 (*FMR1*) gene (Goodlin-Jones *et al.* 2004; Hessl *et al.* 2005). Larger expansions (> 200 repeats; full mutation) generally result in hypermethylation of the *FMR1* gene and subsequent transcriptional silencing. The consequent absence of the *FMR1* protein (FMRP), results in fragile-X syndrome (FXS), which is the most common inherited form of cognitive

Received June 12, 2012; revised manuscript received July 26, 2012; accepted August 14, 2012.

Address correspondence and reprint requests to Isaac N. Pessah, Department of Molecular Biosciences, School of Veterinary Medicine, University of California, Davis, One Shields Avenue, Davis, CA 95616, USA.

E-mail: inpessah@ucdavis.edu

[1]These authors equally contribute to this work.

Abbreviations used: ANTR, anterograde; DIV, days in vitro; *FMR1*, fragile-X mental retardation 1 gene; FMRP, fragile-X mental retardation protein; FXS, fragile-X syndrome; FXTAS, fragile-X-associated tremor/ataxia syndrome; HBSS, Hanks-balanced salt solution; KI, knock-in; OCR, oxygen consumption rate; RETR, retrograde; WT, wild type.

disability, and syndromic form of autism (Jacquemont *et al.* 2007; Hagerman *et al.* 2011). Pre-mutation alleles have estimated frequencies of 1 : 250–810 males and 1 : 130–250 females (Hagerman 2008; Rodriguez-Revenga *et al.* 2009). These pre-mutation carriers can display a range of clinical features that include behavioral and cognitive abnormalities in children (Goodlin-Jones *et al.* 2004; Hessl *et al.* 2005; Farzin *et al.* 2006; Hagerman 2006), primary ovarian insufficiency in about 20% of women (Amiri *et al.* 2008), and a late-onset neurodegenerative disorder, fragile-X-associated tremor/ataxia syndrome (FXTAS) (Tassone *et al.* 2007; Amiri *et al.* 2008; Brouwer *et al.* 2009) in approximately 40% of males (Jacquemont *et al.* 2004). Core clinical features of FXTAS include progressive gait ataxia and intention tremor, often accompanied by cognitive decline and executive dysfunction, peripheral neuropathy, dysautonomia, and Parkinsonism (Berry-Kravis *et al.* 2007; Amiri *et al.* 2008; Bourgeois *et al.* 2009; Brouwer *et al.* 2009).

Pre-mutation carriers display a form of gene dysregulation that is quite distinct from the gene silencing observed with FXS, and which is manifest by substantially increased levels of *FMR1* mRNA, and normal or moderately decreased levels of FMRP. The extent of this altered expression is a function of the size of the CGG-repeat expansion within the pre-mutation range, with larger CGG-repeat expansions associated with higher levels of mRNA and lower levels of protein (Tassone *et al.* 2000). The absence of primary ovarian insufficiency and FXTAS in full mutation patients implies that FMRP deficiency *per se* is not responsible for these pre-mutation disorders. Indeed, evidence from both human and animal studies implicates a direct toxic gain-of-function of pre-mutation CGG (pre-CGG) alleles due to an increase in the CGG-repeat-containing *FMR1* mRNA (Tassone *et al.* 2000; Willemsen *et al.* 2003; Brouwer *et al.* 2007; Sellier *et al.* 2010). Consistent with this hypothesis, characteristic intranuclear inclusions found in neuronal and glial cells of FXTAS cases (Greco *et al.* 2002, 2006) have been demonstrated to contain *FMR1* mRNA but not FMRP (Tassone *et al.* 2004). Moreover, the expanded CGG repeat-RNA is sufficient to form the intranuclear inclusions in both established neural cell lines and primary neural progenitor cells (Arocena *et al.* 2005), as well as in Purkinje neurons (Hashem *et al.* 2009). However, as reduced FMRP levels have been observed in the pre-mutation in both mouse and human; we cannot exclude the possibility that a moderate reduction in FMRP might play a role in modulating some of the pre-mutation phenotypes (Tassone *et al.* 2000; Kenneson *et al.* 2001; Primerano *et al.* 2002; Allen *et al.* 2004; Hunsaker *et al.* 2010, 2011; Peprah *et al.* 2010; Qin *et al.* 2011).

To better understand the mechanistic basis for the pre-mutation disorders, two knock-in (KI) mouse models have been developed to study the developmental onset and progressive neuropathology resulting from pre-mutation CGG expansions. The models were created either by replacing the native 9–10 CGG repeat allele in the homologous *Fmr1* gene with CGG expansions that vary from 100 to > 300 (Berman and Willemsen 2009) or by serially ligating CGG-CCG repeats in exon 1 of the endogenous mouse *Fmr1* gene (Entezam *et al.* 2007). Similar to human pre-mutation carriers, pre-mutation mice with large CGG-repeat expansions exhibit elevated *Fmr1* mRNA and variable reductions in FMRP (Willemsen *et al.* 2003; Brouwer *et al.* 2007). The pre-mutation mouse models display progressive deficits in processing spatial and temporal information, cognitive deficits (Hunsaker *et al.* 2010), motor deficits (Hunsaker *et al.* 2011), and hyperactivity (Qin *et al.* 2011). Ubiquitin-positive intranuclear inclusions, which are neuropathological hallmarks of FXTAS, are also found in pre-mutation mouse neurons and astrocytes (Willemsen *et al.* 2003; Wenzel *et al.* 2010). Early defects in neuronal morphology (Chen *et al.* 2010), migration (Cunningham *et al.* 2011) as well as aberrant spontaneous Ca^{2+} oscillations and clustered burst firing (Cao *et al.* 2012) have been observed in studies of the pre-CGG mouse. The functional abnormalities observed *in vitro* appear to be related, at least in part, from abnormal development of inhibitory (GABAergic) and excitatory (glutamatergic) neuronal networks (D'Hulst *et al.* 2009; Cao *et al.* 2012).

Mitochondria generate the metabolic energy required for neuronal growth and therefore their distribution and dynamics are essential for proper synaptic transmission (Li *et al.* 2004; Hollenbeck and Saxton 2005). Mitochondrial intracellular transport is a dynamic process, which is greatly influenced by Ca^{2+}-dependent processes (Sheng and Cai 2012). Importantly, fibroblasts cultured from human pre-CGG carriers demonstrate decreased complex III and V activities, increased production of reactive oxygen species, and decreased ATP production via oxidative phosphorylation (Ross-Inta *et al.* 2010; Giulivi *et al.* 2011). Decreased levels of a number of mitochondrial proteins were also reported in fibroblast and brain samples from individuals with FXTAS (Ross-Inta *et al.* 2010; Giulivi *et al.* 2011). Recently, the absence of FMRP has been reported to negatively influence the numbers and increase the transport of mitochondria in axons in a *Drosophila* model of FXS (Yao *et al.* 2011). Accordingly, in the present study, we sought to determine whether neurons cultured from pre-CGG KI mice exhibit early alterations in mitochondrial density, transport dynamics, and metabolic function. Alterations in the pre-CGG KI neurons may be similar to those observed in the FXS model; or entirely distinct, reflecting part of the mRNA gain-of-function mechanism believed to underlie FXTAS.

We demonstrate that pre-CGG hippocampal neuronal neurites have significantly decreased mitochondrial density and mobility, as well as aberrant metabolic function. These defects contrast with findings in the FXS model, and are apparent as early as 4 days *in vitro* (DIV). Metabolic

impairments include higher basal oxygen consumption, ATP production, and proton leakage compared with wild type (WT). We conclude that deficits in mitochondrial trafficking and metabolic function occur as a consequence of over-expression of *Fmr1* mRNA, although the moderate reductions of FMRP may play a secondary role. We suggest that the observed mitochondrial dysregulation may contribute to the late-onset pathophysiology observed in pre-mutation carriers and to the risk of developing clinical FXTAS.

Methods

Animals

Experiments were conducted using the expanded CGG trinucleotide repeat (average 170 repeats) knock-in mouse model of the fragile-X pre-mutation. The generation of these mice has been described previously (Willemsen *et al.* 2003). Throughout, male hemizygous pre-mutation and WT mice in the C57BL/6J are used for paired cultures of hippocampal neurons. Breeding a female mouse homozygous for the expanded allele with a male lacking the mutation derived male mice hemizygous for the pre-mutation. Congenic WT male mice were bred with WT females in parallel timed pregnancies. Mice were housed in 12/12-h light-dark cycle with unrestricted access to food and water. All experiments were conducted in compliance with the NIH Guide for Care and Use of Laboratory Animals and were approved by the institutional Animal Care and Use Committee of the University of California at Davis.

Genotyping

DNA was extracted from mouse-tail snips as previously described (Chen *et al.* 2010). The number of CGG repeats were determined by PCR using the Expanded High Fidelity Plus PCR System (Roche Diagnostics, Indianapolis, IN, USA) using forward and reverse primers previously reported (Chen *et al.* 2010). The DNA bands were separated using agarose gels and stained with ethidium bromide to identify their sizes.

Primary hippocampal cultures

Cultures of dissociated hippocampal neurons were prepared by dissection of hippocampi from P1 postnatal mice. Hippocampi were dissected into ice cold Hanks-balanced salt solution (HBSS, Ca^{2+}/Mg^{2+} free; Invitrogen, Carlsbad, CA, USA), and then incubated in HBSS containing trypsin (0.03%) at 37°C for 15 min. Hippocampal tissue was washed three times in warm HBSS, and then triturated with a fire-polished glass pipet. Undissociated tissue fragments were discarded and the remaining cell-containing supernatant was spun down (1100 rpm for 3 min). The cells were resuspended and plated at a density of 10^5 per glass bottom culture dish (MatTek Corporation, Ashland, MA, USA) coated with poly-L-lysine (Peptides International, Louisville, KY, USA) in Neurobasal medium (Invitrogen, Grand Island, NY, USA) containing NS21 supplement (Chen *et al.* 2008), 0.5 mM glutamine, and 5% fetal bovine serum. For measurement of oxygen consumption rate (OCR), the neurons were plated onto XF24 cell culture microplates (Seahorse Bioscience, North Billerica, MA, USA) at a density of 7×10^4 per well. For measuring FMRP and FMR 1 levels, the neurons were plated on 6-well plates at a density of 2×10^6 per well. Four hours after plating, the medium was replaced with serum-free Neurobasal medium containing NS21 supplement and 0.5 mM glutamine. At 2 DIV, the medium was replaced with medium containing fluorodeoxyuridine (30 μM) and uridine (60 μM), to limit the growth of astrocytes. Cells were maintained at 37°C in a humidified environment of ambient air/5% CO_2.

Mitotracker staining and imaging

After hippocampal neurons were allowed to grow to 4 DIV, culture medium was removed and dishes were gently washed with warm HBSS. Neurons were then incubated in staining solution containing 100 nM Mitotracker Red CMXRos (Invitrogen) in HBSS for 20 min at 37°C. HBSS containing dishes were maintained at 37°C while imaging using a micro-incubator (PDMI-2; Warner Instruments, Hamden, CT, USA). Time-lapse images of neurons were acquired every second for 2 min with a 100× objective on an Olympus Ix71 inverted microscope (Olympus, Center Valley, PA, USA). The sequence of images was captured using EasyRatioPro software (Photon Technologies International, Birmingham, NJ, USA). Images were analyzed using Image J (NIH) software to determine mitochondrial density in proximal and distal neurites, as well as number of mitochondria that were mobile or immobile within the entire neurite. Mobile mitochondria were scored as such if they could be clearly resolved traveling at least 1 μm within the 2-min imaging session. Highly mobile mitochondria, which were much less frequently observed, were defined as such if they travelled a distance of 5 μm or greater within the imaging session. All the images were taken and scored with the investigator blinded to the identity of genotype.

Measurements of oxygen consumption rate

A Seahorse Bioscience XF24 Extracellular Flux Analyzer (Seahorse Bioscience) was used to measure the rate change of dissolved O_2 in medium immediately surrounding the neurons cultured in a XF24 cell culture microplate (Seahorse Bioscience). After growing for 4 days, the growth medium was removed and replaced with 675 μL of assay medium pre-warmed to 37°C, composed of Dulbecco's Modified Eagle's Medium without bicarbonate and phenol red (Sigma, St Louis, MO, USA; catalog. no. D5030) supplemented with 31 mM NaCl, 25 mM glucose, 1 mM sodium pyruvate and 2 mM glutamax (pH 7.4). Measurements of OCR were performed after equilibration in assay medium for about 30 min. Briefly, the Seahorse analyzer uses a cartridge with 24 optical fluorescent O_2 and pH sensors that are embedded in a sterile disposable cartridge, 1 for each well. Before each rate measurement, the plungers mix assay media in each well to allow the oxygen partial pressure to reach equilibrium. For measurements of the rates, the plungers gently descend into the wells, forming a chamber that entraps the cells in an approximately 7 μL volume. The O_2 concentration is periodically measured and OCR is obtained from the slopes of concentration change versus time. After the rate measurements, the plungers ascend and the plate is gently agitated to re-equilibrate the medium. OCR is reported in the unit of picomol/min/μg protein. Baseline rates are measured three times. The testing chemicals are pre-loaded in the reagent delivery chambers of the sensor cartridge and then sequentially pneumatically injected into the wells to reach the desired final working concentration. The non-mitochondria OCR

(rotenone insensitive) were subtracted and the averages of three baseline rates and the test rates were used for data analysis.

Western blot

The sample preparation for western blot was performed as described previously (Cao *et al.* 2007). Equal amounts (20 μg) of samples were loaded onto a 10% sodium dodecyl sulfate–polyacrylamide gel electrophoresis gel and transferred to a nitrocellulose membrane by electroblotting. The membranes were blocked with 5% non-skimmed milk in phosphate-buffered saline + 0.1% Tween-20 for 1.5–2 h at 23–27°C. After blocking, membranes were incubated overnight at 4°C in primary antibody dilution (anti-FMRP, 1 : 20 000 and anti-β-actin, 1 : 20 000). The blots were washed and incubated with the IRDye (800CW or 700CW)-labeled secondary antibody (1 : 10 000) for 1 h at 23–27°C. After washing with 0.1% Tween in phosphate-buffered saline for 5 times, the membrane was scanned with the LI-COR Odyssey Infrared Imaging System (LI-COR Biotechnology, Lincoln, NE, USA). The densitometry was performed using LI-COR Odyssey Infrared Imaging System application software 2.1.

Quantitative measurements of *Fmr1* mRNA levels

Total RNA from primary hippocampal cultures was isolated by standard method (Trizol, Ambion Inc., Austin, TX, USA). Precise estimates of *Fmr1* mRNA levels in total RNA were obtained by real time PCR. Details of the method and its application to the study of *Fmr1* mRNAs are described as previously (Tassone *et al.* 2000). The reference gene was β-glucoronidase (*GUS*). Primers and probes were mouse specifics (ABI Assay on Demand, Foster City, CA, USA). The analysis was repeated for three different RNA concentrations, in duplicate, and incorporated standards for each determination to compensate for any changes in reaction efficiency.

Data analysis

Graphing and statistical analysis were performed using GraphPad Prism software (version 5.0; GraphPad Software Inc., San Diego, CA, USA). Statistical significance between different groups was calculated using Student's *t*-test or by an ANOVA and, where appropriate, a Dunnett's Multiple Comparison test. The *p*-values below 0.05% were considered significant.

Results

Western blotting with a chicken monoclonal antibody (Iwahashi *et al.* 2009) detects FMRP in the lysate of neuronal cultures with the major band at 72 kDa (Fig. 1a), a band absent in brain lysates generated from the FMRP knock-out mouse, a model of FXS (data not shown). When normalized to the intensity of β-actin, hippocampal neurons cultured from pre-CGG mice (mean expansion, 170 CGG repeats) express 3.8-fold higher *Fmr1* mRNA levels than observed in 4 DIV WT neurons, whereas FMRP levels are moderately reduced (43 ± 1% of WT levels) (Fig. 1b and c).

Because the distribution of mitochondria along the dendritic processes of neurons is essential for maintaining proper cellular function (Li *et al.* 2004; Hollenbeck and Saxton 2005), we measured the density and dynamics of

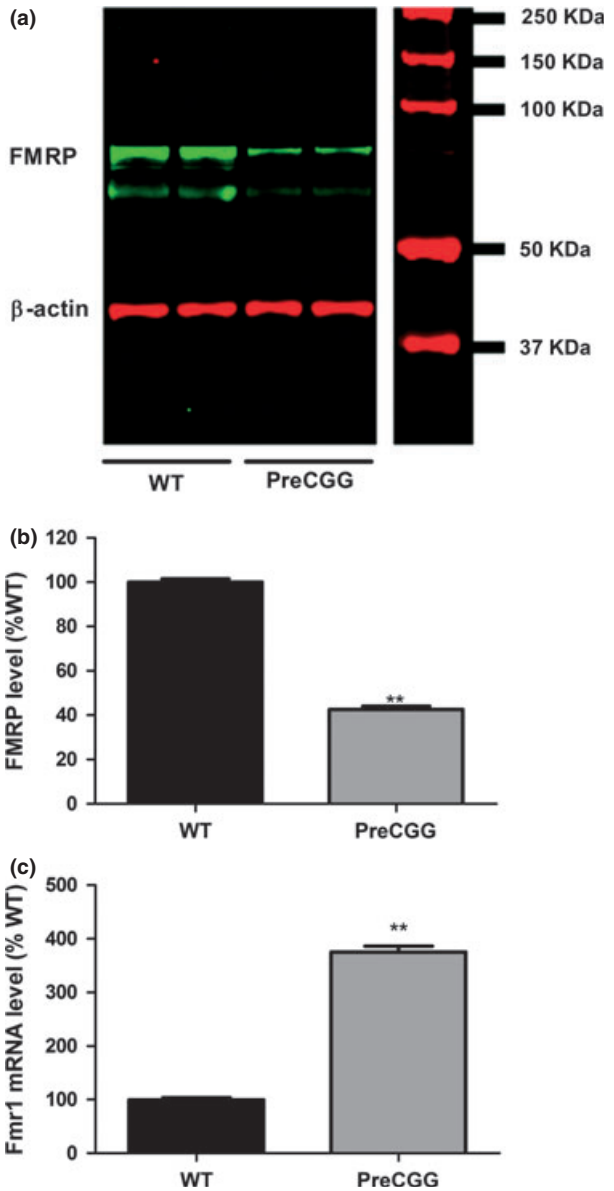

Fig. 1 Pre-mutation cultures express higher levels of *Fmr1* mRNAs with decreased FMRP proteins compared with WT-paired cultures. (a) Representative western blot in paired cultures of WT and pre-CGG hippocampal neurons at 4 DIV. (b) Quantification of FMRP expression level relative to β-actin in paired WT and pre-CGG neuronal cultures at 4 DIV. Data were pooled from two independent cultures. (c) Fmr 1 mRNA comparison between WT and pre-CGG paired neuronal cultures at 4 DIV. Data were pooled from two independent cultures days performed in duplicate. $^{**}p < 0.01$, pre-CGG vs. WT.

mitochondria in neurites of hippocampal neurons. The 4 DIV time point was specifically chosen to permit quantification of mitochondrial density and dynamics at an early stage of neuronal developmental. Densities were evaluated in both the proximal (within 25 μm of the cell soma) and distal (farther than 25 μm from the cell soma) portions of the neurite. The density of mitochondria was significantly reduced in pre-

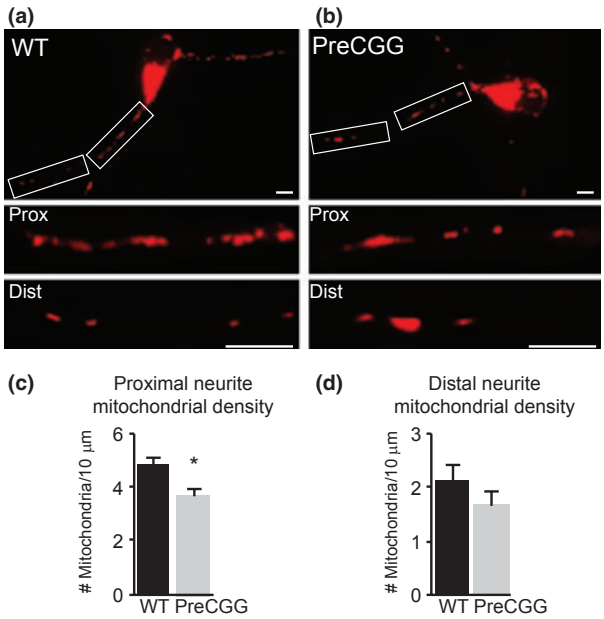

Fig. 2 Decreased mitochondrial density in pre-mutation hippocampal neurites. (a,b) Representative images of WT and pre-CGG 4 DIV hippocampal neurons labeled with Mitotracker dye. Below whole cell images are higher magnification images of proximal (within 25 μm of soma) and distal (farther than 25 μm from soma) neurites. (c) Number of mitochondria was decreased in pre-CGG proximal neurites by 25% (3.67 ± 0.32 pre-CGG vs. 4.88 ± 0.29 WT, $p = 0.01$), WT $n = 98$ neurites from 53 cells, pre-CGG $n = 53$ neurites from 33 cells. (d) The number of mitochondria in distal neurites showed a trend toward fewer mitochondria in pre-CGG neurites, but this was not statistically significant (1.68 ± 0.25 pre-CGG vs. 2.12 ± 0.32 WT, $p = 0.338$). WT $n = 66$ neurites from 49 cells, pre-CGG $n = 41$ neurites from 24 cells. *$p = 0.01$. Scale bars represent 5 μm.

CGG proximal neurites (3.67 ± 0.32 pre-CGG versus 4.88 ± 0.29 WT, #mitochondria/10 μm, $p = 0.01$). The distal neurites showed a trend toward fewer mitochondria as well, but the reduction was not statistically significant ($p = 0.338$) (Fig. 2). The movement of mitochondria was also investigated by the acquisition of time-lapse images, which allowed for the tracking of individual mitochondria over the course of the imaging session (Fig. 3a and b). The mitochondria that maintained their position throughout the imaging session were referred to as 'immobile', whereas mitochondria that traveled at least 1 μm within the 2-min imaging session were classified as 'mobile'; mitochondria that traveled a distance of 5 μm or greater within the imaging session were termed 'highly mobile'. The 'highly mobile' mitochondria were also evaluated for the direction of their movement. Direction was scored as anterograde (ANTR), retrograde (RETR), or moving in both directions (Both).

A strong deficit in the dynamics of mitochondrial movement was apparent in the neurites from pre-CGG neurons compared with WT neurons. Although the number of immobile mitochondria was not significantly different between the two genotypes, the number of mobile mitochondria in pre-CGG neurons was significantly reduced (1.21 ± 0.15 pre-CGG versus 2.36 ± 0.15 WT, no. mitochondria/10 μm, $p < 0.01$) (Fig. 3c and d). The discrepancy in mobility between pre-CGG and WT neurons was especially apparent in the number of mitochondria that traveled a great distance. Highly mobile mitochondria numbers were significantly reduced (0.16 ± 0.04 pre-CGG versus 0.47 ± 0.06 WT, no. mitochondria/10 μm, $p < 0.01$) in the neurites of pre-CGG neurons compared with those of WT (Fig. 3e). Similar results were obtained when the data were normalized relative to total number of mitochondria (mobile + immobile) for each of the proximal and distal dendrites (Figure S1). The percentage of highly mobile mitochondria that moved in an ANTR, RETR, or in Both directions, was not significantly different between genotypes (Fig. 3f). Highly mobile mitochondria in both pre-CGG and WT neurons more commonly moved in the retrograde direction, with a smaller percentage of mitochondria moving ANTR or in Both directions (Fig. 3a, b and f).

The oxygen consumption rate (OCR) of mitochondria from intact 4 DIV hippocampal neurons was measured in real time, using a Seahorse Bioscience XF24 extracellular flux analyzer (Seahorse Bioscience). Hippocampal neurons from pre-mutation mice displayed a 23.0 ± 2.9% higher ($p < 0.01$) basal OCR compared with their WT counterpart (Fig. 4a and b). The oligomycin-sensitive OCR, which is related to ATP production, was 17.1 ± 2.8% higher ($p < 0.01$) in pre-CGG neurons than that measured with WT neurons, suggesting that pre-CGG neurons produced more ATP than WT. The oligomycin-insensitive OCR, which reflects proton leakage, was 43.2 ± 4.8% higher ($p < 0.01$) than that of WT neurons. The maximal OCR in both genotypes was also evaluated in the presence of the uncoupling agent FCCP (1 μM). FCCP stimulated OCRs were comparable to respective basal levels in both genotypes. This suggests that in our dissociated neuronal system, the spare respiratory capacity is small. This is consistent with the previous report in which FCCP (1 μM) treatment led to little stimulation in a hippocampal slice preparation (Schuh *et al.* 2011). However, the maximal OCR was higher in pre-CGG compared with WT neurons (17.1 ± 5.5% higher than WT, $p < 0.05$).

Discussion

Males with *FMR1* pre-mutation have reduced hippocampal activation during memory recall tasks, presumably because of dysfunction in the posterior hippocampus, which also correlated with psychological symptoms (Koldewyn *et al.* 2008). Anxiety-related problems are also common both prior to and after the onset of FXTAS, and appear to be related to hippocampal changes (Adams *et al.* 2009). High levels of *FMR1* mRNA have been demonstrated in the hippocampus of human patients (Tassone *et al.* 2004) where ubiquitin

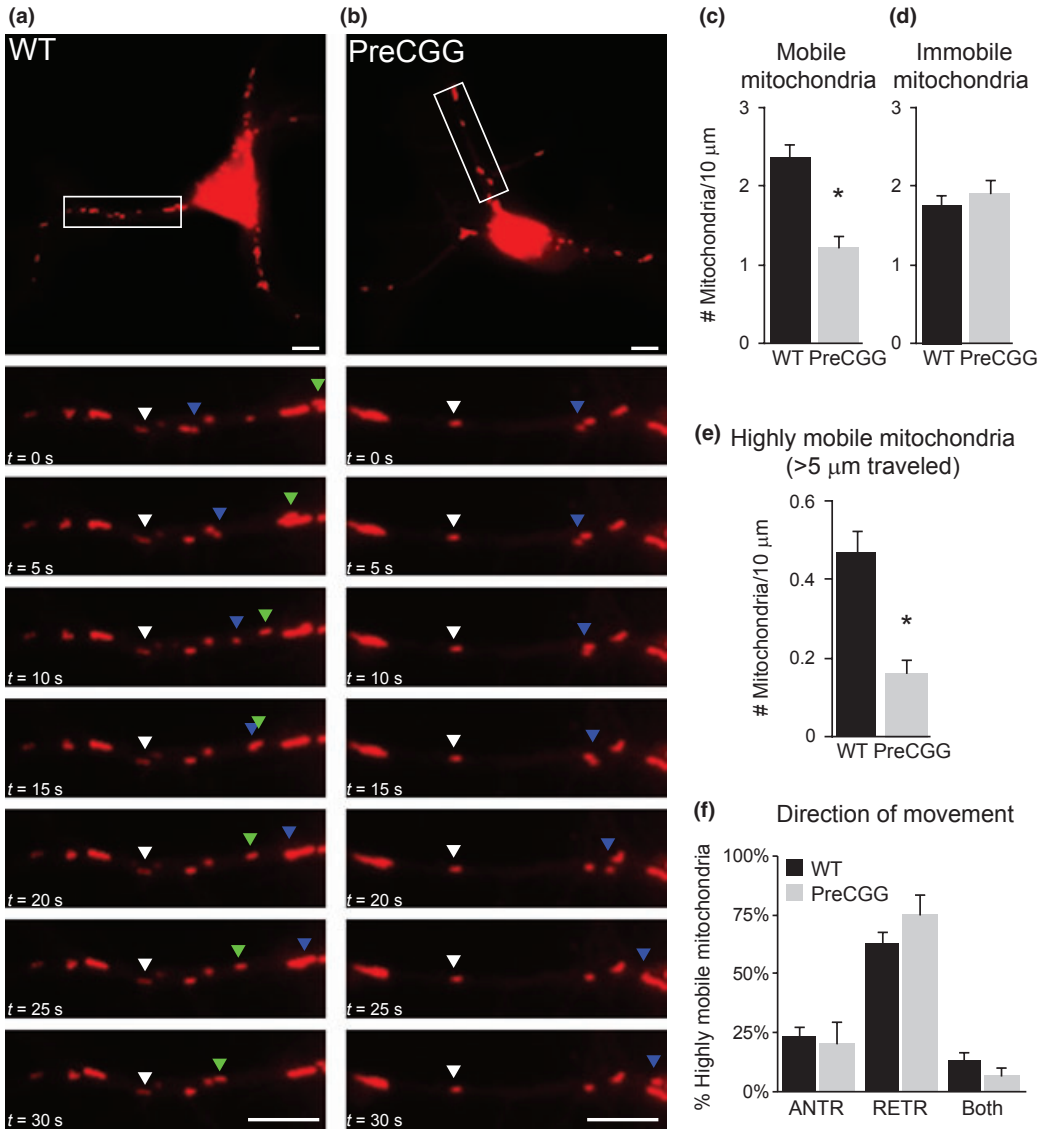

Fig. 3 Decreased mitochondrial motility in pre-mutation neurons. (a, b) Representative images of WT and pre-CGG 4 DIV hippocampal neurons labeled with Mitotracker dye. Below whole cell images are higher magnification time lapse images of mitochondrial movement in neurites. Labeled examples are shown of immobile (white arrowhead) as well as anterogradely (green arrowhead) and retrogradely (blue arrowhead) moving mitochondria. (c) Number of mobile mitochondria was decreased in pre-CGG neurons by 48% compared with WT (1.21 ± 0.15 pre-CGG vs. 2.36 ± 0.15 WT, $p < 0.01$). (d) Number of immobile mitochondria was not significantly different between pre-CGG and WT neurons (1.91 ± 0.17 pre-CGG vs. 1.76 ± 0.12 WT, $p = 0.47$). (e) Number of highly mobile mitochondria, was decreased in pre-CGG neurons by 66% compared with WT (0.16 ± 0.04 pre-CGG vs.0.47 ± 0.06 WT, $p < 0.01$). (f) The direction of travel of highly mobile mitochondria was not significantly different between pre-CGG and WT neurons. Both showed similar percentage of mitochondria moving ANTR, RETR, or both directions (Both). ANTR: 0.20 ± 0.09 pre-CGG vs. 0.23 ± 0.04 WT, $p = 0.693$. RETR: 0.74 ± 0.09 pre-CGG vs. 0.63 ± 0.05 WT, $p = 0.276$. BOTH: 0.06 ± 0.03 pre-CGG vs. 0.13 ± 0.03 WT, $p = 0.239$. WT $n = 98$ neurites from 53 cells, pre-CGG $n = 53$ neurites from 33 cells. *$p < 0.01$. Scale bars represent 5 μm.

positive inclusions appear in 10–40% of the hippocampal neurons (Greco *et al.* 2002, 2006), findings modeled by the knock-in pre-mutation mouse used in the present study (Wenzel *et al.* 2010).

In this study, we have shown abnormalities in both mitochondrial trafficking and mitochondrial bioenergetics in hippocampal neurons from a mouse model of FXTAS as early as 4 DIV. The density and intracellular trafficking of mitochondria in neurites were significantly reduced in 4 DIV pre-CGG mouse hippocampal neurons. The pre-CGG neurons also displayed higher basal OCR, proton leakage, and higher ATP production. The findings presented here are of

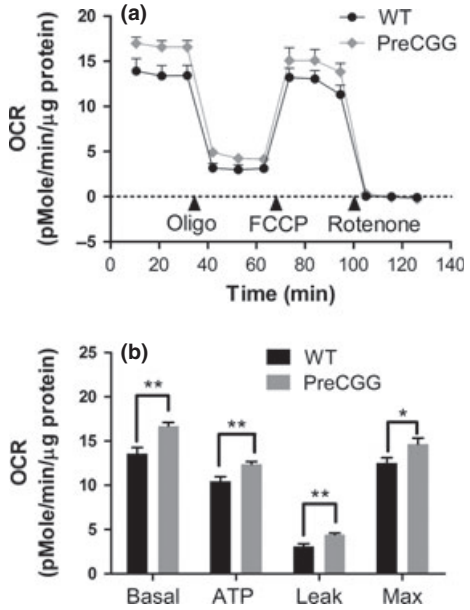

Fig. 4 Bioenergetics in WT and pre-CGG neurons. (a) Time-response relationships for oxygen consumption before and after addition of oligomycin (1 μM), FCCP (1 μM) and rotenone (1 μM) in both genotypes. The non-mitochondrial OCR determined by addition of rotenone (1 μM) was subtracted. (b) Quantification of basal, ATP production, proton leak, and maximal OCR in WT and pre-CGG 4DIV hippocampal neurons. In pre-CGG neurons, the basal OCR was 23% higher (16.71 ± 0.40 pmol/min/μg protein, $n = 36$) compared with WT neurons (13.58 ± 0.68 pmol/min/μg protein, $n = 30$, $^{**}p < 0.01$). ATP production in pre-CGG neurons was 17% higher (12.27 ± 0.29 pmol/min/μg protein, $n = 30$) than observed in WT neurons (10.48 ± 0.48 pmol/min/μg protein, $n = 36$, $^{**}p < 0.01$). Proton leak was 43% higher (4.44 ± 0.15 pmol/min/μg protein, $n = 30$) compared with WT neurons (3.1 ± 0.28 pmol/min/μg protein, $n = 36$, $^{**}p < 0.01$). Maximal OCR was 17% higher in pre-CGG neurons (14.67 ± 0.69 pmol/min/μg protein, $n = 30$) than observed for WT neurons (12.53 ± 0.58 pmol/min/μg protein, $n = 36$, $^{*}p < 0.05$).

particular interest considering the increasing evidence linking mitochondrial defects and neurodegenerative disorders (Pickrell and Moraes 2010). These mitochondrial deficits in pre-CGG neurons occur in the presence of elevated *Fmr1* mRNA and moderately reduced FMRP levels, in accord with previous findings in brain lysates and neuronal cultures from KI mice expressing pre-CGG repeats (Hollenbeck and Saxton 2005; Brouwer *et al.* 2007, 2008a,b) and with findings from human pre-mutation carriers and FXTAS patients (Tassone *et al.* 2000, 2004). Therefore, the presence of both significantly elevated *Fmr1* mRNA and intermediate levels of FMRP reflects the human pre-CGG molecular phenotype (Tassone *et al.* 2000, 2004), thus distinguishing pre-CGG hippocampal neurons from those of FXS models. These abnormalities in the density and mobility of mitochondria may contribute to the altered pattern of neuronal complexity reported previously using the same *in vitro* pre-CGG model, where the dendritic complexity in pre-CGG hippocampal neurons was decreased as early as 7 DIV (Chen *et al.* 2010). Moreover, such mitochondrial deficits may contribute to migration defects (Cunningham *et al.* 2011), reduced dendritic branching, and altered spine length observed *in vivo* in the pre-CGG mouse neocortex (Berman *et al.* 2012).

Recently, it was reported in a *Drosophila* model of FXS (Yao *et al.* 2011) that the numbers of axonal mitochondria were inversely correlated with FMRP level. Observed increases in the number of mitochondria were caused specifically by the loss of FMRP, and neuronal overexpression of FMRP led to lowered mitochondrial numbers. These observations stand in direct contrast to the observed decreases in mitochondrial number and dynamics in the pre-CGG KI mouse; suggesting that *Fmr1* mRNA toxicity resulting from the ~4-fold increased RNA levels, not the moderately reduced FMRP levels, is likely responsible for the current mitochondrial phenotype in pre-mutation mice. This conclusion is supported by the recent observation that the variation of FMRP among individuals in the general population (normal *FMR1* alleles) is greater than four-fold, despite the absence of any clinical features of fragile-X pre-mutation-associated disorders (Iwahashi *et al.* 2009; Lessard *et al.* 2011).

In conclusion, we demonstrate that pre-CGG hippocampal neurons show abnormalities in the number, mobility, and metabolic function of mitochondria. Pre-mutation hippocampal neurons displayed higher basal oxygen consumption, ATP production, as well as higher proton leakage. The deficits in mitochondrial trafficking and metabolic function may contribute to pathophysiology in pre-mutation carriers and may constitute a risk factor of developing clinical FXTAS.

Acknowledgements

We thank Yucui Chen for her guidance regarding dissociated hippocampal cultures and Diptiman Bose for helpful discussions regarding imaging. We thank Binh Ta for carrying out all of the genotyping and Lee Rognlie-Howes for coordinating the breeding of mice used in this study. This work was supported by NIH grants DE019583 (PJH), AG032119 (PJH, INP), ES04699, ES011269 and the J.B. Johnson Foundation (INP), and NS062411 (RFB). Eitan S. Kaplan, Zhengyu Cao, Susan Hulsizer, and Flora Tassone performed experiments; all authors analyzed the data and drafted the manuscript. Isaac N. Pessah and Paul J. Hagerman designed the experiments, evaluated raw data and data summaries. Robert Berman laboratory supplied the time-mated mice. All authors edited the manuscripts. The authors have no interest to declare.

Supporting information

Additional supporting information may be found in the online version of this article:

Figure S1. Mobile and Highly Mobile Fraction of Total Mitochondria.

As a service to our authors and readers, this journal provides supporting information supplied by the authors. Such materials are peer-reviewed and may be re-organized for online delivery, but are not copy-edited or typeset. Technical support issues arising from supporting information (other than missing files) should be addressed to the authors.

References

Adams P. E., Adams J. S., Nguyen D. V. *et al.* (2009) Psychological symptoms correlate with reduced hippocampal volume in fragile X premutation carriers. *Am. J. Med. Genet. B Neuropsychiatr. Genet.* **153B**, 775–785.

Allen E. G., He W., Yadav-Shah M. and Sherman S. L. (2004) A study of the distributional characteristics of FMR1 transcript levels in 238 individuals. *Hum. Genet.* **114**, 439–447.

Amiri K., Hagerman R. J. and Hagerman P. J. (2008) Fragile X-associated tremor/ataxia syndrome: an aging face of the fragile X gene. *Arch. Neurol.* **65**, 19–25.

Arocena D. G., Iwahashi C. K., Won N., Beilina A., Ludwig A. L., Tassone F., Schwartz P. H. and Hagerman P. J. (2005) Induction of inclusion formation and disruption of lamin A/C structure by premutation CGG-repeat RNA in human cultured neural cells. *Hum. Mol. Genet.* **14**, 3661–3671.

Berman R. F. and Willemsen R. (2009) Mouse models of fragile x-associated tremor ataxia. *J. Investig. Med.* **57**, 837–841.

Berman R. F., Murray K. D., Arque G., Hunsaker M. R. and Wenzel H. J. (2012) Abnormal dendritic and spine morphology in primary visual cortex in the CGG knock-in mouse model of the fragile X premutation. *Epilepsia* **53**, 149–159.

Berry-Kravis E., Abrams L., Coffey S. M. *et al.* (2007) Fragile X-associated tremor/ataxia syndrome: clinical features, genetics, and testing guidelines. *Mov. Disord.*, **22**, 2018–2030, quiz 2140.

Bourgeois J. A., Coffey S. M., Rivera S. M. *et al.* (2009) A review of fragile X premutation disorders: expanding the psychiatric perspective. *J. Clin. Psychiatry* **70**, 852–862.

Brouwer J. R., Mientjes E. J., Bakker C. E., Nieuwenhuizen I. M., Severijnen L. A., Van der Linde H. C., Nelson D. L., Oostra B. A. and Willemsen R. (2007) Elevated Fmr1 mRNA levels and reduced protein expression in a mouse model with an unmethylated Fragile X full mutation. *Exp. Cell Res.* **313**, 244–253.

Brouwer J. R., Huizer K., Severijnen L. A., Hukema R. K., Berman R. F., Oostra B. A. and Willemsen R. (2008a) CGG-repeat length and neuropathological and molecular correlates in a mouse model for fragile X-associated tremor/ataxia syndrome. *J. Neurochem.* **107**, 1671–1682.

Brouwer J. R., Severijnen E., de Jong F. H., Hessl D., Hagerman R. J., Oostra B. A. and Willemsen R. (2008b) Altered hypothalamus-pituitary-adrenal gland axis regulation in the expanded CGG-repeat mouse model for fragile X-associated tremor/ataxia syndrome. *Psychoneuroendocrinology* **33**, 863–873.

Brouwer J. R., Willemsen R. and Oostra B. A. (2009) The FMR1 gene and fragile X-associated tremor/ataxia syndrome. *Am. J. Med. Genet. B Neuropsychiatr. Genet.* **150B**, 782–798.

Cao Z., George J., Baden D. G. and Murray T. F. (2007) Brevetoxin-induced phosphorylation of Pyk2 and Src in murine neocortical neurons involves distinct signaling pathways. *Brain Res.* **1184**, 17–27.

Cao Z., Hulsizer S., Tassone F., Tang H. T., Hagerman R. J., Rogawski M. A., Hagerman P. J. and Pessah I. N. (2012) Clustered burst firing in FMR1 premutation hippocampal neurons: amelioration with allopregnanolone. *Hum. Mol. Genet.* **21**, 2923–2935.

Chen Y., Stevens B., Chang J., Milbrandt J., Barres B. A. and Hell J. W. (2008) xml: re-defined and modified supplement B27 for neuronal cultures. *J. Neurosci. Methods* **171**, 239–247.

Chen Y., Tassone F., Berman R. F., Hagerman P. J., Hagerman R. J., Willemsen R. and Pessah I. N. (2010) Murine hippocampal neurons expressing Fmr1 gene premutations show early developmental deficits and late degeneration. *Hum. Mol. Genet.* **19**, 196–208.

Cunningham C. L., Martinez Cerdeno V., Navarro Porras E. *et al.* (2011) Premutation CGG-repeat expansion of the Fmr1 gene impairs mouse neocortical development. *Hum. Mol. Genet.* **20**, 64–79.

D'Hulst C., Heulens I., Brouwer J. R., Willemsen R., De Geest N., Reeve S. P., De Deyn P. P., Hassan B. A. and Kooy R. F. (2009) Expression of the GABAergic system in animal models for fragile X syndrome and fragile X associated tremor/ataxia syndrome (FXTAS). *Brain Res.* **1253**, 176–183.

Entezam A., Biacsi R., Orrison B., Saha T., Hoffman G. E., Grabczyk E., Nussbaum R. L. and Usdin K. (2007) Regional FMRP deficits and large repeat expansions into the full mutation range in a new Fragile X premutation mouse model. *Gene* **395**, 125–134.

Farzin F., Perry H., Hessl D. *et al.* (2006) Autism spectrum disorders and attention-deficit/hyperactivity disorder in boys with the fragile X premutation. *J. Dev. Behav. Pediatr.* **27**, S137–S144.

Giulivi C., Ross-Inta C., Omanska-Klusek A., Napoli E., Sakaguchi D., Barrientos G., Allen P. D. and Pessah I. N. (2011) Basal bioenergetic abnormalities in skeletal muscle from ryanodine receptor malignant hyperthermia-susceptible R163C knock-in mice. *J. Biol. Chem.* **286**, 99–113.

Goodlin-Jones B. L., Tassone F., Gane L. W. and Hagerman R. J. (2004) Autistic spectrum disorder and the fragile X premutation. *J. Dev. Behav. Pediatr.* **25**, 392–398.

Greco C. M., Hagerman R. J., Tassone F., Chudley A. E., Del Bigio M. R., Jacquemont S., Leehey M. and Hagerman P. J. (2002) Neuronal intranuclear inclusions in a new cerebellar tremor/ataxia syndrome among fragile X carriers. *Brain* **125**, 1760–1771.

Greco C. M., Berman R. F., Martin R. M. *et al.* (2006) Neuropathology of fragile X-associated tremor/ataxia syndrome (FXTAS). *Brain* **129**, 243–255.

Hagerman R. J. (2006) Lessons from fragile X regarding neurobiology, autism, and neurodegeneration. *J. Dev. Behav. Pediatr.* **27**, 63–74.

Hagerman P. J. (2008) The fragile X prevalence paradox. *J. Med. Genet.* **45**, 498–499.

Hagerman R., Au J. and Hagerman P. (2011) FMR1 premutation and full mutation molecular mechanisms related to autism. *J. Neurodev. Disord.* **3**, 211–224.

Hashem V., Galloway J. N., Mori M., Willemsen R., Oostra B. A., Paylor R. and Nelson D. L. (2009) Ectopic expression of CGG containing mRNA is neurotoxic in mammals. *Hum. Mol. Genet.* **18**, 2443–2451.

Hessl D., Tassone F., Loesch D. Z. *et al.* (2005) Abnormal elevation of FMR1 mRNA is associated with psychological symptoms in individuals with the fragile X premutation. *Am. J. Med. Genet. B Neuropsychiatr. Genet.* **139B**, 115–121.

Hollenbeck P. J. and Saxton W. M. (2005) The axonal transport of mitochondria. *J. Cell Sci.* **118**, 5411–5419.

Hunsaker M. R., Goodrich-Hunsaker N. J., Willemsen R. and Berman R. F. (2010) Temporal ordering deficits in female CGG KI mice heterozygous for the fragile X premutation. *Behav. Brain Res.* **213**, 263–268.

Hunsaker M. R., von Leden R. E., Ta B. T., Goodrich-Hunsaker N. J., Arque G., Kim K., Willemsen R. and Berman R. F. (2011) Motor deficits on a ladder rung task in male and female adolescent and adult CGG knock-in mice. *Behav. Brain Res.* **222**, 117–121.

Iwahashi C., Tassone F., Hagerman R. J., Yasui D., Parrott G., Nguyen D., Mayeur G. and Hagerman P. J. (2009) A quantitative ELISA assay for the fragile x mental retardation 1 protein. *J. Mol. Diagn.* **11**, 281–289.

Jacquemont S., Hagerman R. J., Leehey M. A. *et al.* (2004) Penetrance of the fragile X-associated tremor/ataxia syndrome in a premutation carrier population. *JAMA* **291**, 460–469.

Jacquemont S., Hagerman R. J., Hagerman P. J. and Leehey M. A. (2007) Fragile-X syndrome and fragile X-associated tremor/ataxia syndrome: two faces of FMR1. *Lancet Neurol.* **6**, 45–55.

Kenneson A., Zhang F., Hagedorn C. H. and Warren S. T. (2001) Reduced FMRP and increased FMR1 transcription is proportionally associated with CGG repeat number in intermediate-length and premutation carriers. *Hum. Mol. Genet.* **10**, 1449–1454.

Koldewyn K., Hessl D., Adams J., Tassone F., Hagerman P. J., Hagerman R. J. and Rivera S. M. (2008) Reduced hippocampal activation during Recall is associated with elevated FMR1 mRNA and psychiatric symptoms in men with the Fragile X premutation. *Brain Imaging Behav.* **18**, 105–116.

Lessard M., Chouiali A., Drouin R., Sebire G. and Corbin F. (2011) Quantitative measurement of FMRP in blood platelets as a new screening test for fragile X syndrome. *Clin. Genet.* doi: 10.1111/j.1399-0004.2011.01798.x.

Li Z., Okamoto K., Hayashi Y. and Sheng M. (2004) The importance of dendritic mitochondria in the morphogenesis and plasticity of spines and synapses. *Cell* **119**, 873–887.

Peprah E., He W., Allen E., Oliver T., Boyne A. and Sherman S. L. (2010) Examination of FMR1 transcript and protein levels among 74 premutation carriers. *J. Hum. Genet.* **55**, 66–68.

Pickrell A. M. and Moraes C. T. (2010) What role does mitochondrial stress play in neurodegenerative diseases? *Methods Mol. Biol.* **648**, 63–78.

Primerano B., Tassone F., Hagerman R. J., Hagerman P., Amaldi F. and Bagni C. (2002) Reduced FMR1 mRNA translation efficiency in fragile X patients with premutations. *RNA* **8**, 1482–1488.

Qin M., Entezam A., Usdin K., Huang T., Liu Z. H., Hoffman G. E. and Smith C. B. (2011) A mouse model of the fragile X premutation: effects on behavior, dendrite morphology, and regional rates of cerebral protein synthesis. *Neurobiol. Dis.* **42**, 85–98.

Rodriguez-Revenga L., Madrigal I., Pagonabarraga J., Xuncla M., Badenas C., Kulisevsky J., Gomez B. and Mila M. (2009) Penetrance of FMR1 premutation associated pathologies in fragile X syndrome families. *Eur. J. Hum. Genet.* **17**, 1359–1362.

Ross-Inta C., Omanska-Klusek A., Wong S. *et al.* (2010) Evidence of mitochondrial dysfunction in fragile X-associated tremor/ataxia syndrome. *Biochem. J.* **429**, 545–552.

Schuh R. A., Clerc P., Hwang H., Mehrabian Z., Bittman K., Chen H. and Polster B. M. (2011) Adaptation of microplate-based respirometry for hippocampal slices and analysis of respiratory capacity. *J. Neurosci. Res.* **89**, 1979–1988.

Sellier C., Rau F., Liu Y. *et al.* (2010) Sam68 sequestration and partial loss of function are associated with splicing alterations in FXTAS patients. *EMBO J.* **29**, 1248–1261.

Sheng Z. H. and Cai Q. (2012) Mitochondrial transport in neurons: impact on synaptic homeostasis and neurodegeneration. *Nat. Rev. Neurosci.* **13**, 77–93.

Tassone F., Hagerman R. J., Taylor A. K., Gane L. W., Godfrey T. E. and Hagerman P. J. (2000) Elevated levels of FMR1 mRNA in carrier males: a new mechanism of involvement in the fragile-X syndrome. *Am. J. Hum. Genet.* **66**, 6–15.

Tassone F., Iwahashi C. and Hagerman P. J. (2004) FMR1 RNA within the intranuclear inclusions of fragile X-associated tremor/ataxia syndrome (FXTAS). *RNA Biol.* **1**, 103–105.

Tassone F., Adams J., Berry-Kravis E. M., Cohen S. S., Brusco A., Leehey M. A., Li L., Hagerman R. J. and Hagerman P. J. (2007) CGG repeat length correlates with age of onset of motor signs of the fragile X-associated tremor/ataxia syndrome (FXTAS). *Am. J. Med. Genet. B Neuropsychiatr. Genet.* **144B**, 566–569.

Wenzel H. J., Hunsaker M. R., Greco C. M., Willemsen R. and Berman R. F. (2010) Ubiquitin-positive intranuclear inclusions in neuronal and glial cells in a mouse model of the fragile X premutation. *Brain Res.* **1318**, 155–166.

Willemsen R., Hoogeveen-Westerveld M., Reis S. *et al.* (2003) The FMR1 CGG repeat mouse displays ubiquitin-positive intranuclear neuronal inclusions; implications for the cerebellar tremor/ataxia syndrome. *Hum. Mol. Genet.* **12**, 949–959.

Yao A., Jin S., Li X., Liu Z., Ma X., Tang J. and Zhang Y. Q. (2011) Drosophila FMRP regulates microtubule network formation and axonal transport of mitochondria. *Hum. Mol. Genet.* **20**, 51–63.